Forcing of Atlantic Equatorial and Subpolar Millennial Cycles by Precession

Andrew McIntyre* and Barbara Molfino†

Abundance cycles of the marine alga *Florisphaera profunda* centered on a period of 7600 carbon-14 years (8400 calendar years) are present in high-resolution records from the equatorial Atlantic spanning 0 to 45,000 years ago. These cycles correlate with Heinrich events 1 through 5, which document rapid changes in continental ice melting around the subpolar North Atlantic. These variations in *F. profunda* are a direct response to modulation in zonal wind-driven divergence produced by a precessional component of orbital variation during a time of reduced eccentricity modulation.

Heinrich events are millennial-scale pulses of ice-rafted detritus that punctuate the last glacial record in the high-latitude North Atlantic (*1*) and indicate rapid melting of adjacent continental ice. These pulses either are a response to or result in climate change recorded by other last glacial climate proxies (*2*). Millennial-scale response of the atmosphere-ocean system has also been documented far from the North Atlantic (*3*). In this report we describe such millennial-scale signals from the equatorial Atlantic and address three questions: Do these low-latitude events correlate with Heinrich events? Are these signals cyclic? Do they share a common cause?

The signal is the abundance of the Coccolithophoridae species *Florisphaera profunda*, expressed as a percentage relative to all other Coccolithophoridae species. Unlike all other Coccolithophoridae species that produce a fossil record, *F. profunda* is restricted to the lower euphotic zone. In the equatorial Atlantic, the control on *F. profunda*'s relative abundance is the thermocline-nutricline gradient, which is a direct function of wind-forced current velocity (*4*). A decrease in the zonal wind shear of the tropical easterlies decreases South Equatorial Current (SEC) flow, which decreases divergence, nutrients, and primary production in the shallow euphotic zone. Hence, production of all other coccolithophorids is reduced relative to *F. profunda*. An increase in zonal wind shear produces the opposite effect. This cause-and-effect relation has been documented for annual and orbital forcing (*5*).

We studied three large-volume gravity cores from the east side of the mid-Atlantic ridge, all sited above the modern lysocline (*6*): RC2402, 0°34.0′N, 13°39.0′W, at a depth of 3837 m; RC2408, 1°20.0′S, 11°54.0′W, at a depth of 3885 m; and RC2417, 5°3.0′S, 10°11.0′W, at a depth of 3530 m. All sites lie within the equatorial region of maximum seasonal divergence and heat flux centered on 10°W (*7*, *8*). Core RC2402 is at the northern edge, RC2417 is at the southern edge, and RC2408 is on the axis of SEC flow; thus, the strongest signal of seasonal divergence and its long-term variation is in RC2408. Core siting results in mean sedimentation rates of 4.5 cm per thousand years (ky) for RC2402, 8 cm/ky for RC2408, and 3.0 cm/ky for RC2417. Cores were sampled at 2-cm intervals, which yielded mean resolutions of 440 years for RC2402, 250 years for RC2408, and 670 years for RC2417. Piston cores RC2401, RC2407, and RC2416, from the same sites, have chronologies established by oxygen isotope stratigraphy and CLIMAP/SPECMAP age models (*5*). We obtained a series of accelerator mass spectrometry (AMS) ^{14}C ages for cores RC2402 and RC2408 (Table 1). These and extant AMS ^{14}C ages for RC2417 (*9*) were used to refine the chronologies transferred from the piston cores. These ages establish a chronology in ^{14}C years, uncalibrated for reservoir effect, of 0 to 40,000 years ago (ka), in RC2402, 0 to 36 ka in RC2408, and 0 to 18 ka in RC2417.

Temporal variations in the percentage of *F. profunda* (Fig. 1) depict both a long-period signal of high amplitude and a short-period signal of low amplitude. Our focus is on the long-period signal (Fig. 1A), which is characterized by a series of well-defined maxima and minima, particularly evident in RC2408. We computed the ages of maxima 1 through 5 (labeled with Arabic numerals) in ^{14}C years by (i) the dating of maxima samples (RC2408), (ii) interpolation between AMS controlled levels, or (iii) intercore correlation (Table 2). We computed the ages of maxima 6 and older from oxygen isotope chronology. To emphasize the long-period component and simplify intercore comparison (see the legend to Fig. 1), we smoothed all three signals with moving average filters (Fig. 1B). Spectral analysis of these signals shows power centered on 7.0 ky for RC2402, 7.8 ky for RC2408, and 9.5 ky for RC2417 (Fig. 1D). The variation in mean period is due in part to differences in the length of the record. Because only the youngest five maxima have ages controlled by AMS ^{14}C ages, our analysis involves only the interval from 0 to 36.9 ^{14}C ka.

Core RC2408 has the best age control, so the other two cores have been truncated accordingly. Spectral analysis (*10*) of the truncated signals demonstrated that dominant power (not illustrated) is centered on 7.5 ky for RC2402 and 7.6 ky for RC2417, essentially the same as the dominant power center for RC2408.

Maxima and minima define the range of system response. Of equal importance is defining when the system changed. The concept of a semitransitive climate that remains in one mode until forcing, a threshold energy, accelerates the system into a new modality (*11*) is applicable. System changes are denoted by the points of maximum acceleration in the signal, depicted by the minimum in the first derivative *d*Fp/

Table 1. AMS ^{14}C dates from monospecific samples of *Neogloboquadrina dutertrei* for cores RC2402 and RC2408. Calendric ages for RC2408 were used in erecting the core chronology. N.A., not applicable.

NOSAM no.	Depth (cm)	^{14}C age (years)	± Error	Calendar age (years)
		Core RC2402		
OS-5488	12	5,880	30	
OS-5490	16	7,500	30	
OS-5489	20	8,950	30	
OS-5492	24	10,100	35	
OS-5491	32	12,200	40	
OS-5493	40	12,850	40	
OS-5497	56	15,350	50	
OS-5494	72	18,000	60	
OS-5496	84	20,200	65	
OS-5504	100	22,100	150	
OS-5495	125	28,700	110	
OS-5498	175	40,100	420	
		Core RC2408		
OS-6804	14.5	7,230	40	7,633
OS-6805	56.5	13,550	50	15,669
OS-3931*	60	13,700	60	15,888
OS-3935*	64	14,300	70	16,731
OS-3930*	68	14,400	70	16,792
OS-3937*†	72	13,900	55	N.A.
OS-3936†	77	14,150	110	N.A.
OS-3938	82	16,500	65	18,975
OS-4144†	87	14,550	65	N.A.
OS-3933*†	92	13,700	70	N.A.
OS-3934	97	18,050	100	21,027
OS-6806	130.5	20,700	75	24,250
OS-3929	134	20,800	80	N.A.
OS-6807	178.5	27,400	110	32,550
OS-3932	180	28,200	140	33,500
OS-6808	224.5	32,700	160	39,000
OS-4144	230	35,200	340	41,000

*AMS ^{14}C dates from monospecific samples of *Globigerinoides ruber*. †Data rejected as anomalously young.

Lamont-Doherty Earth Observatory of Columbia University, Palisades, NY 10964, USA.

*To whom correspondence should be addressed.
†Present address: Central Intelligence Agency, Washington, DC 20505, USA.

dt, the rate of change of *F. profunda* with time (Roman numerals, Fig. 1C), and henceforth referred to as inflection points. These inflection points precede the corresponding *F. profunda* maxima (ages in Table 2). First derivatives of the truncated interval were spectrally analyzed after the signals had been smoothed with an 11-point filter to suppress centennial-scale and enhance millennial-scale periods. All cores have dominant power centered on 7.6 ky (Fig. 1E).

Maxima 2, 3, 4, 5, and 7 in the percentages of *F. profunda* have ages that correlate with Heinrich event ages 1 through 5, respectively, within their associated errors (Table 2). The *F. profunda* values constitute continuous signals not limited to a glacial. They contain more maxima than the documented Heinrich events. If *F. profunda* is responding to the same forcing in the system as the Heinrich events, then there should be some indication of Heinrich-like events at ~7, 44, and 58 ka. There is evidence for high-latitude response at ~7 ka (*12*) and 44 ka (*13*, *14*), but these are not Heinrich events in the strict sense.

We converted the RC2408 record, which has the highest accumulation rates and the best ^{14}C control, to calendric years using the calibration of Stuiver and Reimer (*15*) for ages <19 ka and that of Bard *et al.* (*16*) for ages >19 ka (*14*). As RC2408 is sited in tropical waters, only the 400-year correction factor of the referenced calibrations was applied (Table 1 and Fig. 2).

The conversion yielded a temporal distribution that exhibits greater regularity of *F. profunda* maxima ages, particularly between those peaks (1 to 3) occurring within the interval characterized by the greatest discrepancy between ^{14}C and calendric ages (Table 2). In addition, the conversion shows that the *F. profunda* signal is symmetric: The mean deviation from perfect symmetry is 3.4% (*17*), which is within the error envelope attributable to chronology. Heinrich (ocean-record) and Dansgaard-Oeschger (ice-record) events are asymmetric.

Spectral analysis of the calendric signal yields power concentrated at 8.4, 1.4, and 0.7 ky for the unmodified signal. As in the ^{14}C chronology, we have smoothed the signal. Spectral analysis after smoothing (not depicted) yielded a single peak centered on a period of 8.4 ky that accounts for 53% of the total variance (*18*). Visual and statistical proof of cyclicity is evident when a series of independent bandpass filters is applied to the modified signal. Each filter has

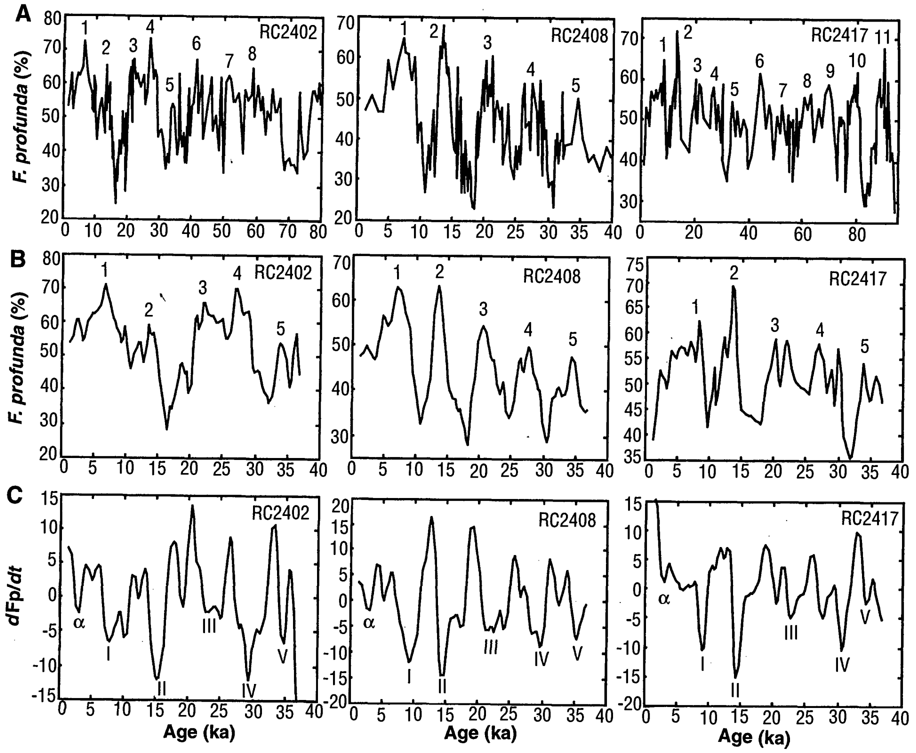

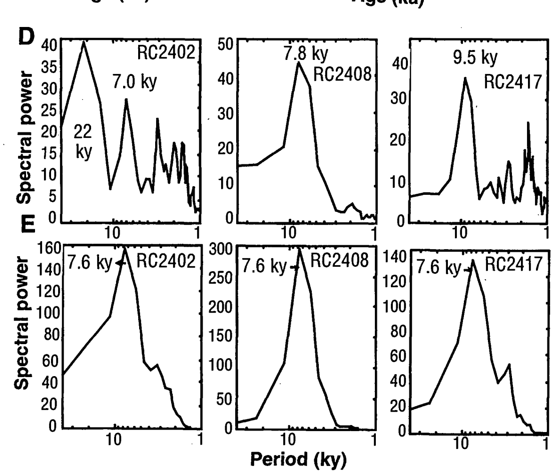

Fig. 1. Bivariate plots of the percentage of *F. profunda* in the ^{14}C time domain and selected spectral signatures. (**A**) Signals of the full-length records. (**B**) Signals resampled at 0.3 ky and then smoothed with a filter appropriate to the resolution of each core and chosen both to enhance millennial-scale periods >3 ky and to produce signals with equivalent definition for intercore comparison. These are five-, seven-, and three-point moving-average filters for cores RC2402, RC2408, and RC2417, respectively. RC2402 and RC2417 were truncated at 36.9 ka to match RC2408 because this is the interval controlled by AMS ^{14}C ages. Maxima in *F. profunda* are indicated by Arabic numerals; ages are given in Table 2. (**C**) The first derivative of the truncated signals smoothed with an 11-point filter. Inflection points, indicated by Roman numerals, are related to and precede the corresponding maxima (Arabic numerals); ages are in Table 2. (**D**) Linear spectra of the full-length record shown in (A). Although all contain power at or near 7.5 ky ^{14}C, the longer records are dominated by longer periods. (**E**) Linear spectra of the first derivative of the truncated signals in (C); all have power centered on 7.6 ky ^{14}C.

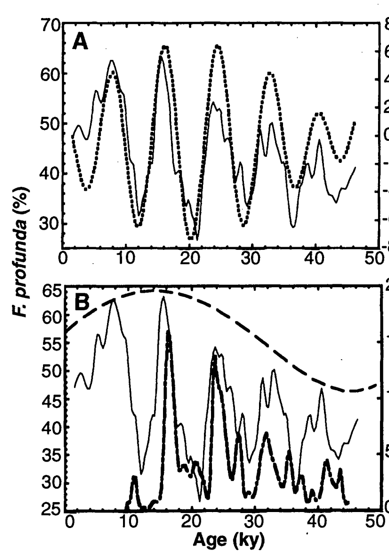

Fig. 2. (**A**) Core RC2408 *F. profunda* signal [solid line in both (A) and (B)] smoothed with a seven-point filter plotted to calendar age (see text) compared to the "best fit" bandpass filter (heavy dashed line) with a mean period of 8.4 ky. The correlation (*r*) is 0.87. (**B**) *Florisphaera profunda* signal compared with the number of lithic fragments per gram in core V2381 (dark dotted line). Lithic maxima denote Heinrich events 1 through 4. Eccentricity, the percentage of ellipticity in the orbit of the earth (long-dashed line, value not included on the *y* axis), is a direct control of precession modulation.

the same bandwidth but differs in central period from 7.4 to 9.4 ky in increments of 0.1 ky. The filtered output with the best overall fit to the signal (Fig. 2A) has a wavelength of 8.4 ky, a correlation coefficient of 0.84, a squared coherency of 0.939, and a phase of $-1.9° \pm 10°$. No other filtered output had as good a fit in all three criteria.

Heinrich events defined by peaks of ice-rafted detritus are documented in the North Atlantic in core V2381 (*19*). We transposed these data to calendric chronology using the same methods as those that were applied to the RC2408 *F. profunda* signal. We statistically resampled V2381 at 0.3 ky and smoothed with a three-point filter for comparison with RC2408 (Fig. 2B). The two signals have the same number of peaks, although only Heinrich events 1, 2, and 3 are coincident with *F. profunda* maxima 2, 3, and 4, respectively. Heinrich event 4 and *F. profunda* maximum 5 are offset, a chronology problem. As important as the peak-to-peak match is the match of amplitude envelopes, which we consider additional circumstantial evidence of a common cause. Spectral analysis of V2381 lithic fragments yielded a dominant peak centered on 8.4 ky. Cross-spectral analysis between the two signals yielded a squared coherency of 0.81 for this period: The two signals have essentially the same modulation. This is proof of correlation, not coincidence. The *F. profunda* signal leads with a phase of $21.7° \pm 18.0°$, which is marginally statistically significant and, given chronologic constraints, is not an indicator of mechanism.

We documented that the *F. profunda* signal is a direct response to forcing at the annual and precessional periods by the mechanism of insolation-forced variation in wind-controlled divergence (*5*). In the tropics, primary precessional components centered on 22 and 19 ky are the dominant forcing, but there are harmonic periods with values of 11 and 9.5 ky. The zonal intensity of the tropical easterlies is modulated by the strength of the North African monsoon, which attains a seasonal maximum in Northern Hemisphere summer. In the tropics, the sun passes overhead twice in the year (*20, 21*). Over one precessional cycle, this produces two intervals during which perihelion is coincident with the solstice in Northern Hemisphere summer and thus two times when maximum meridionality and minimum zonality of the tropical easterlies occur. This is what produces the 11- and 9.5-ky periods in the equatorial signals (*20, 21*).

We consider the 8.4-ky period a variant of this mechanism for the following reasons. First, when the entire signal of RC2402 and RC2417, 81 and 93 ka, respectively, is spectrally analyzed, the dominant period is centered on ~10 ky. As we sequentially truncated these signals by eliding older intervals in 10-ky units, the dominant period shifted from ~10 to 8.4 ky when the record was <60 ka. Second, the variance-amplitude envelope of both the *F. profunda* signal in RC2408 and the lithic fragment signal in V2381 matches that of eccentricity (Fig. 2). Chronologic error is insufficient to permit the 8.4-ky period to be the 9.5-ky period (*22*).

The nonlinear response of climate to insolation forcing produces combination tones of the primary orbital components, which are present as secondary periods of lower amplitude in the geologic record (*23*). The primary orbitals that control low-latitude insolation are precession and eccentricity; the latter causes variation in the total annual insolation received and, more important, modulates precessional insolation. For example, as eccentricity decreases, there is a decrease in both total energy (small) received and seasonal variation in energy (large) in the tropics. About 60 ka, eccentricity amplitude decreased rapidly to a nadir at 46 ka. The low-amplitude eccentricity period has a wavelength of only 72 ky (46 ka to 27 ky in the future) (*24*). The mean period of 8.43 ky (*18*) is half of the additive combination tone 16.85 ky produced by the 72-ky eccentricity and the 22-ky precession component. We stress that tropical insolation since ~60 ka is atypical of the preceding 300 ky, when high-amplitude long-wave eccentricity maximized modulation of precession. This effect is documented by equatorial sea surface temperature depicting a change in rhythm at ~60 ka (*5*).

We propose that the equatorial signals and the high-latitude signals from the North Atlantic are linked in both forcing and mechanism. The presence of a well-developed *F. profunda* maximum (maximum 1) in the Holocene at a time when there was insufficient ice to produce a Heinrich event indicates that our system is not controlled by high-latitude mechanisms. Forcing is low-latitude precessional insolation at both the primary and secondary periods. The mechanism is variation in the zonality of the low-latitude forcing winds, which directly affects advection of low-latitude surface water heat to the high-latitude North Atlantic. This mechanism differs from the mechanism that operates by high-latitude control of thermohaline flow, modulated by processes that alter the stability of surface oceanography in the regions of thermohaline initiation (*25*). Our hypothesis relies on energy from that portion of the Earth that runs the terran system and in which small variations in received energy per unit area translate into major changes in the total energy of the system.

The mechanism we hypothesize is analogous to a long-period El Niño. The Atlantic's hot-water reservoir lies within the Caribbean and Gulf of Mexico, centered on 15° and 25°N with mean dynamic heights of 5.6 and 5.5, respectively. These dynamic heights represent a relief of ~1 m above the Atlantic at the same latitude and ~2 m above the subpolar North Atlantic. When the tropical easterlies diminish (*F. profunda* maxima), the warm waters are released from this reservoir. Unlike outflow in the Pacific,

Table 2. Mean ages (in ka) of maxima in the percentages of *F. profunda* (Arabic numerals) and inflection points (Roman numerals), compared to Heinrich events. Ages through numeration 5/V in RC2402 and RC2408 and 3/III in RC2417 are interpolated values between AMS ^{14}C ages. Ages of older events are estimated from isotope chronology. Heinrich ages are from Bond and Lotti (*19*) or Fronval *et al*. (*13*) and Porter and Zhisheng (*14*). Calendric ages only are given for RC2408. N.A., not applicable.

F. profunda events	RC2402	RC2408	RC2408 (calendric)	RC2417	Heinrich events (*19*)	Heinrich events (*13, 14*)
α	3.00 ± 0.03	3.00 ± 0.03	3.0	3.00 ± 0.03	N.A.	
1	6.89 ± 0.04	7.20 ± 0.04	7.5	7.21 ± 0.04	None?	
I	7.7	9.3	10.2	9.0		
2	13.71 ± 0.06	13.57 ± 0.06	15.6	13.6 ± 0.06	14.3	
II	15.5	14.4	16.8	14.4		
3	22.08 ± 0.15	20.46 ± 0.09	24.2	21.1 ± 0.15	20.5	
III	23.9	21.3	27.7	22.8		
4	26.6 ± 0.11	27.7 ± 0.13	32.1	27.0 ± 0.13	26.7	
IV	28.3	29.7	35.4	30.6		
5	34.8 ± 0.35	34.5 ± 0.34	40.5	33.9 ± 0.42	35.5	32.7
V	36.8	35.4	41.4	39.0		
6	43.7 ± 1.50			44.1 ± 2.50	None	43.5
7	51.3 ± 2.50			52.3 ± 3.50	49.9	51.0
8	58.9 ± 3.50			59.0 ± 3.50	None	58.0

the outflow in the Atlantic cannot be eastward along the equatorial corridor because there is no direct oceanographic connection. Instead, these warm saline waters flow eastward into the western boundary current of the North Atlantic subtropical gyre and are delivered into the subpolar Atlantic, producing the rapid melting of ice and hence Heinrich events. This is a seasonal process. From inflection points to maxima, there is a diminution in the zonal component relative to the meridional component of the tropical easterlies in the key season of Northern Hemisphere summer. Relaxation of the zonal force permits increasing amounts of heat and salt to flow eastward into the western boundary current, culminating in *F. profunda* maxima and Heinrich events. This mechanism alters the partitioning of heat loss from these inland seas. Latent heat flux to the atmosphere decreases relative to sensible heat loss to the North Atlantic Ocean by means of surface water advection as the zonality of tropical easterlies decreases; the opposite effect occurs as the zonality increases.

The mechanism that we propose for the delivery of heat- and salt-enhancing or -retarding continental ice accumulation and sea ice–ocean density stratification is complimentary to the "binge and purge hypothesis" (*26*), to the "conveyer belt hypothesis" (*25*), and to the evidence that variation in the advection of warm Atlantic surface water into the Norwegian Sea influenced both atmospheric circulation through the last glacial-interglacial transition (*27*) and Greenland ice for 0 to 41 ka (*2*). Our results also support the initial view that Heinrich events were a product of precessional forcing (*1*). Circumstantial evidence exists in the correlation between Heinrich events and similar millennial-scale responses in the Greenland ice (*19*) and with spectral analyses of Vostock (Antarctica) and GRIP (Greenland) ice cores, which contain stable spectral peaks at 8.96 and 7.76 ky, respectively (*28*).

If our scenario is correct, then at ~3 ^{14}C ka, equivalent to ~3 ka (α in Fig. 1C), the modality of the system changed. During this time, there was a concomitant increase in precipitation around the North Atlantic in subpolar latitudes and a decrease in precipitation in West Africa (*29–32*). The precessional forcing and response mechanism described here will continue to at least 28,000 A.D.; consequently, *F. profunda* maxima should occur at ~3200 A.D. and ~11,600 A.D.

REFERENCES AND NOTES

1. H. Heinrich, *Quat. Res.* **29**, 143 (1988).
2. P. Mayewski *et al.*, *Science* **263**, 1747 (1994).
3. A. T. Kotilainen and N. J. Shackleton, *Nature* **377**, 323 (1995); E. C. Grimm, G. L. Jacobson Jr., W. A. Watts, B. C. S. Hansen, K. A. Maasch, *Science* **261**, 198 (1993).
4. B. Molfino and A. McIntyre, *Science* **249**, 766 (1990).
5. A. McIntyre *et al.*, *Paleoceanography* **4**, 19 (1989); A. McIntyre *et al.*, *Program for the Fifth International Conference on Paleoceanography* (Halifax, Nova Scotia, 1995), p. 54.
6. D. J. Verardo and A. McIntyre, *Paleoceanography* **9**, 63 (1994).
7. G. Reverdin, in *Upwelling in the Ocean: Modern Processes and Ancient Records*, C. P. Summerhayes *et al.*, Eds. (Wiley, New York, 1995), pp. 125–148.
8. R. H. Weisberg and T. Y. Tang, *J. Geophys. Res.* **92**, 3709 (1987).
9. G. A. Jones, *Deep-Sea Res.*, in press.
10. G. M. Jenkins and D. G. Watts, *Spectral Analysis and Its Applications* (Holden-Day, Oakland, CA, 1968). All spectra are linear variances of time series calculated by standard time series procedures at the 95% confidence interval: linear detrending; prewhitening (0.8); autocovariance function; Tukey-Hanning lag window ($M = n/3$); time interval, 0.3 ky, and a fixed n (132 for ^{14}C and 147 for calendric signals) for all three cores.
11. E. N. Lorenz, *Meteorol. Monogr.* **8**, 1 (1968).
12. L. D. Keigwin and G. A. Jones, *Paleoceanography* **10**, 973 (1995).
13. T. Fronval *et al.*, *Nature* **374**, 443 (1995).
14. S. C. Porter and A. Zhisheng, *ibid.* **375**, 305 (1995).
15. M. Stuiver and P. J. Reimer, *Radiocarbon* **35**, 215 (1993).
16. E. Bard *et al.*, *ibid.*, p. 191.
17. Test of symmetry of a random variable Y about a point c. If we assume that Y has a frequency function p, then symmetry about c is $p(Y + c) = p(Y - c)$. P. J. Bickel and K. A. Doksum, *Mathematical Statistics* (Holden-Day, Oakland, CA, 1977).
18. Calendric chronology of cores RC2402 and RC2408 yields eight peak-to-peak intervals having a range of 8.1 to 9.0 ky, with a mean of 8.43 ky.
19. G. C. Bond and R. Lotti, *Science* **267**, 1005 (1995).
20. D. A. Short *et al.*, *Quat. Res.* **35**, 157 (1991).
21. T. K. Hagelberg *et al.*, *Paleoceanography* **9**, 545 (1994).
22. The error of estimate in years for the AMS ^{14}C chronology ranges from ±30 to ±420 for dated samples, but for interpolated values we consider that these estimates could be larger as a result of variation in sedimentation rate. However, in RC2408, *F. profunda* maxima were either directly AMS-dated or have dates closely allied with them. Calendric conversion yields 2σ errors ranging from ±35 to ±450. We found that the extreme case for the oldest peak-to-peak interval for conversion (*15*), using a minus error for the younger peak and a plus error for the older peak, is 8.75 ky. The estimate of the oldest interval for conversion (*16*) is 9.3 ky.
23. A. Berger, *Quat. Int.* **2**, 1 (1989); P. I. Pestiaux *et al.*, *Clim. Change* **12**, 9 (1988).
24. A. Berger and M. F. Loutre, *Sci. Rep. Inst. Astron. Geophys.* **13**, 1 (1988).
25. W. S. Broecker *et al.*, *Clim. Dyn.* **6**, 265 (1992).
26. H. Haflidason *et al.*, *Geology* **23**, 1059 (1995).
27. D. R. MacAyeal, *Paleoceanography* **8**, 775 (1993).
28. P. Yiou *et al.*, *Geophys. Res. Lett.* **22**, 2175 (1995).
29. B. Fontaine and S. Bigot, *Int. J. Climatol.* **13**, 271 (1993).
30. F. Gasse and E. vanCampo, *Earth Planet. Sci. Lett.* **126**, 435 (1994). Evidence of increased drought in West Africa at ~4 to 3 ka is presented.
31. D. A. Hodell *et al.*, *Nature* **375**, 391 (1995). In their figure 2, there is a marked change in lithic-chemical-isotope character of the lake sediments at ~3 ka (^{14}C years) in Central America.
32. S. P. Harrison *et al.*, *Quat. Res.* **45**, 138 (1996); S. O. Dahl and A. Nesje, *Holocene* **3**, 269 (1993). Increased precipitation is inferred from changes in vegetation and lake levels and glacial accretion on the continents adjacent to the subpolar North Atlantic after 5 ka.

33. We thank M. Yarusinski for assistance. Supported by NSF [MG&G grant OCE93-13821 (95%)], and NSF OCE801015 AMS/National Ocean Sciences Accelerator Mass Spectrometry Facility. This is Lamont-Doherty Earth Observatory contribution 5579.

9 July 1996; accepted 25 September 1996

Latest *Homo erectus* of Java: Potential Contemporaneity with *Homo sapiens* in Southeast Asia

C. C. Swisher III, W. J. Rink, S. C. Antón, H. P. Schwarcz, G. H. Curtis, A. Suprijo, Widiasmoro

Hominid fossils from Ngandong and Sambungmacan, Central Java, are considered the most morphologically advanced representatives of *Homo erectus*. Electron spin resonance (ESR) and mass spectrometric U-series dating of fossil bovid teeth collected from the hominid-bearing levels at these sites gave mean ages of 27 ± 2 to 53.3 ± 4 thousand years ago; the range in ages reflects uncertainties in uranium migration histories. These ages are 20,000 to 400,000 years younger than previous age estimates for these hominids and indicate that *H. erectus* may have survived on Java at least 250,000 years longer than on the Asian mainland, and perhaps 1 million years longer than in Africa. The new ages raise the possibility that *H. erectus* overlapped in time with anatomically modern humans *(H. sapiens)* in Southeast Asia.

The geologic age and taxonomic affinity of hominid fossils from Ngandong and Sambungmacan, Central Java, bear directly on the controversy surrounding the origin of anatomically modern humans (*H. sapiens*). Proponents of a regional continuity model for the origin of *H. sapiens* consider that these fossils are both morphologically and temporally transitional between Javanese *H. erectus*, such as Sangiran 17, that are older than 780,000 years ago (ka), and early robust Australian *H. sapiens*, such as Willandra Lakes Hominid (WLH) 50, that first appear about 30 ka (*1*, *2*). The opposing view is that *H. sapiens* arose in Africa less than 200 ka and only recently spread out